

Global Photometric Properties of Barred Galaxies

Kouji Ohta

Department of Astronomy, Kyoto University, Kyoto, 606-01 Japan

Abstract. Global photometric properties of barred galaxies are reviewed based on the surface photometry of barred galaxies.

1. Introduction

Surface photometry of barred galaxies offers information on the luminosity distribution of bars, disks, and bulges, which are the basic knowledge for the understanding of the structure and the origin of bars. These data are also indispensable for comparison with models of barred galaxies and with simulations dealing with bar formation. Until the seventies, there had been only several barred galaxies which were studied in detail (e.g., Crane 1975; Benedict 1976; Okamura & Takase 1976; Okamura 1978). In the eighties and the nineties, detailed surface photometry of barred galaxies was made extensively (e.g., Blackman 1983; Duval & Athanassoula 1983; Duval & Monnet 1985; Elmegreen & Elmegreen 1985; Pence & de Vaucouleurs 1985; Buta 1986, 1987; Ann 1986; Baumgart & Peterson 1986; Ohta, Hamabe, & Wakamatsu 1990; Odewahn 1991; Wozniak & Pierce 1991). In this review I present properties of the surface brightness distribution of barred galaxies mainly based on our work.

Our sample of barred galaxies consists of six typical early-type (SB0 - SBab) and three late-type (SBcd - SBd) barred galaxies. The early-type barred galaxies were taken in *B*-band and details for the early-type barred galaxies are described in Ohta et al. (1990). For the late-type barred galaxies, *I*-band images were taken using the 188-cm telescope at the Okayama Astrophysical Observatory (NAOJ) with a CCD, because the surface brightness in the *I*-band does not suffer so much from the contamination by star formation and dust lanes.

2. Azimuthal profiles

Figure 1 shows examples of the azimuthal profiles of the barred galaxies extracted along concentric ellipses which should appear as circles centered on the nuclei in the planes of the galaxies. The most notable feature is that the profiles in the bar regions are not simply sinusoidal in early-type barred galaxies; the bar component seems to be a hump on the flat profile. In the late-type galaxies, the profiles are close to sinusoidal. This situation is more clearly shown in Fourier decomposition.

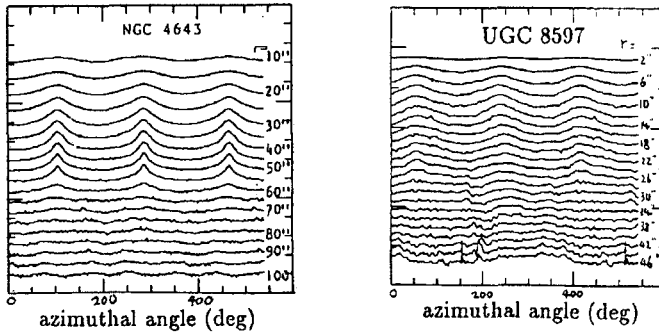


Figure 1. Azimuthal profiles of an early-type (left panel) and a late-type (right panel) barred galaxy. The ordinate and the abscissa are surface brightness in arbitrary units and azimuthal angle, respectively. The upper part in each panel shows profiles in the bulge region, the middle part shows profiles in the bar region, and the lower part shows profiles in the outer disk region.

Figure 2 shows the results of the Fourier decomposition. The Fourier components are defined as follows,

$$I(r, \theta) = A_0(r)/2 + \sum_m [A_m(r) \cos m\theta + B_m(r) \sin m\theta],$$

where

$$A_m(r) = \frac{1}{\pi} \int_0^{2\pi} I(r, \theta) \cos m\theta d\theta, \quad \text{and} \quad B_m(r) = \frac{1}{\pi} \int_0^{2\pi} I(r, \theta) \sin m\theta d\theta.$$

The Fourier amplitude of the m -th component is defined as

$$I_0(r) = A_0(r)/2, \quad I_m(r) = [A_m(r)^2 + B_m(r)^2]^{1/2},$$

and the relative amplitude of the m -th component is defined as $I_m(r)/I_0(r)$. In both early- and late-type barred galaxies, the amplitudes of the $m=2$ component are the largest, but in the early-type barred galaxies the contributions of $m=4$, $m=6$, and $m=8$ components are also large, while in the late-type barred galaxies only the amplitudes of $m=4$ are significant and contributions from higher components are negligible.

3. Radial profiles

Figure 3 shows examples of the azimuthally averaged radial surface brightness distribution together with the distribution along the bar major axis and bar minor axis.

The azimuthally averaged profiles are very similar to those of unbarred galaxies and basically consist of a quarter-law bulge and an exponential disk. In fact, the distribution of the scale lengths and the central/effective surface

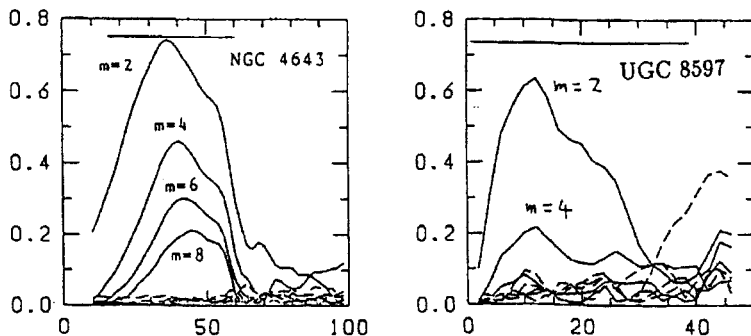


Figure 2. Relative Fourier amplitude of an early-type (left panel) and a late-type (right panel) barred galaxy. The ordinate is the relative amplitude of the Fourier component and the abscissa is radius in arcsec. A horizontal line in each panel represents a bar region.

brightnesses of disks and bulges of barred galaxies is quite similar to those of unbarred galaxies. Kodaira et al. (1986) derived the scale lengths and the surface brightnesses of 167 galaxies in the Virgo cluster and Ursa Major clouds by decomposing the galaxies into spheroid and disk components based on a homogeneous data set using the same analysis method. There is no significant difference in the distribution of these parameters between barred galaxies and unbarred galaxies.

Next we examine the profiles along the bar major axis. In the early-type barred galaxies, the surface brightness distributions in the bar regions are flat as compared with those in the outer disks, and sharp luminosity cut-offs are seen at the bar ends. The e-folding scale of the cut-off ranges from 0.4 to 1.7 kpc. In the late-type barred galaxies, the situation is quite different: the slopes of the profiles in the bar regions are larger than those in the outer disks and no cut off is seen at the bar ends. The presence of these two types of bars, that is, flat bar and exponential bar, was first noticed by Elmegreen & Elmegreen (1985) when they examined the profiles along bars and spiral arms. The flat bars tend to reside in early-type galaxies and exponential bars in late-type galaxies.

4. Properties of bars

4.1. Bar length

The ratio of a bar length to a disk scale length or size tends to decrease from early-type to late-type barred galaxies, which is also pointed out by Martin (1995); the ratio is about three times larger in early-type barred galaxies than in late-type barred galaxies. The bar length also correlates with a bulge size (Athanasoula & Martinet 1980). Martin (1995) confirms the correlation and gives the relation, $l_{\text{bar}}/D_0 = 2.34(d_{\text{bulge}}/D_0) - 0.03$, where l_{bar} is the deprojected length of a bar, d_{bulge} is the diameter of a bulge, and D_0 is the apparent major isophotal diameter at $\mu = 25 \text{ mag arcsec}^{-2}$.

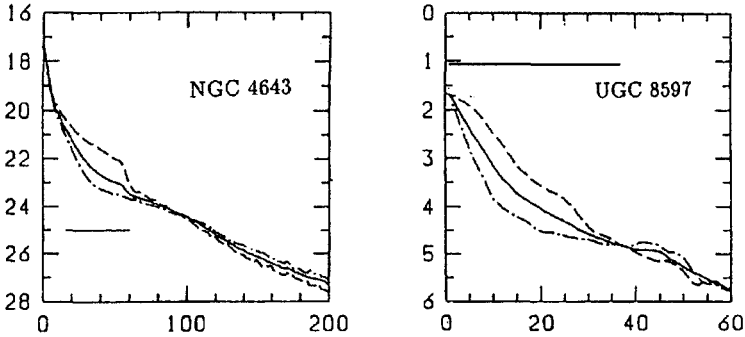


Figure 3. Radial profiles of an early-type (left panel) and a late-type (right panel) barred galaxy. The ordinate is surface brightness in magnitude scale and the abscissa is radius in arcsec. Solid lines, dashed lines, and dot-dashed lines represent azimuthally averaged profiles, profiles along the bar major axis, and profiles along the bar minor axis, respectively. A horizontal line in each panel shows the bar region.

4.2. Luminosity distribution of a bar

The definition of a bar component is not clear. We proposed a definition of a bar component (Ohta et al. 1990). As can be seen in Figure 1, interbar regions on the azimuthal profiles are broad and nearly flat, whereas the bar regions protrude prominently above them as sharp and narrow humps. So the bar appears to be a non-axisymmetric component superposed on the underlying axisymmetric component. In other words, the disks of barred galaxies can be decomposed expediently into an axisymmetric component and non-axisymmetric component. From a physical point of view, there may be no axisymmetric component in the disks of real barred galaxies, because stellar orbits must deviate significantly from circular orbits by the presence of a bar potential. However, this decomposition can extract the bar and non-axisymmetric component explicitly. Simple subtraction of the interbar profile from the original image of a galaxy does not appropriately reproduce the luminosity distribution of the bar itself. Thus an iteration process using a fitting by a model bar described below is necessary to derive the bar component itself. Two examples of the resulting bar components in the early-type barred galaxies are shown in Figure 4. The most prominent feature of the bar component is that the contours of it are not ellipses; rather they are close to rectangular shapes, except for obvious features of spiral arms, though the shape may depend on the bulge structure.

The luminosity distribution along the major axis and parallel to the minor axis of the bar component derived above is well represented by an exponential function and a Gaussian function, respectively. That is, the intensity distribution of the bar itself is,

$$I(x, y) = I(0, 0)\exp(-x/x_0)\exp(-(y/y_0)^2),$$

with a sharp cut off at the bar end. This form of function was also proposed by Blackman (1983) for a late-type barred galaxy, but he fitted the model to

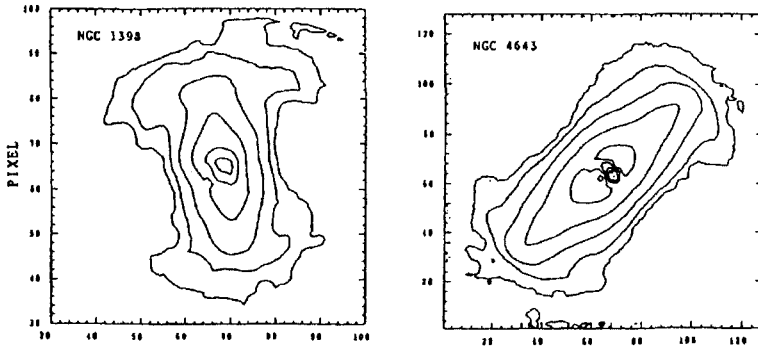


Figure 4. Examples of the isophotal map of the bar component itself in the early-type barred galaxies (NGC 1398 and NGC 4643). The outermost contour is $25.0 \text{ mag arcsec}^{-2}$, and the interval is $1.0 \text{ mag arcsec}^{-2}$.

the observed bar directly. An ellipsoid having a density distribution of $\rho = \rho_0[1 - (x/a)^2 - (y/b)^2 - (z/c)^2]^n$ is often used for models of the bar component. When we adopt this type of density distribution, the fitting to the observed bars is good for the bar major axis profiles, but very poor for the bar cross profiles.

For the shape of bars, Athanassoula et al. (1990) proposed the following expression:

$$\left(\frac{|x|}{a}\right)^c + \left(\frac{|y|}{b}\right)^c = 1.$$

When $c = 2$ the shape is elliptical, and if $c < 2$ and $c > 2$ the shape is disk-like and boxy, respectively. This expression also reproduces the observed isophotes of the bars well. There are two parameters, c and $\frac{b}{a}$; they may be good indicators of discriminating morphology between barred galaxies and unbarred galaxies.

4.3. Luminosity fraction of a bar

Elmegreen & Elmegreen (1985) proposed a clear method of defining the luminosity fraction of a bar. They defined it using the amplitudes of the Fourier components of the azimuthal profiles as $(I_2 - I_4)/I_0$. To compare with this method, we derived the luminosity fraction of the bar by integrating the total intensity in the region between bulge radius and bar length and by integrating the bar component itself derived above in the same region. The resulting values are about 30 to 50% in the early-type barred galaxies. The result agrees with that derived from the Fourier amplitudes, though the values are closer when we include a higher component. The luminosity fraction of the bar within R_{25} is also defined using the above bar luminosity fraction. It ranges from about 10 to 30% in early-type and from a few to 10% in late-type barred galaxies (Elmegreen & Elmegreen 1985; Ohta et al. 1990).

4.4. Symmetry of a bar

Bars have straight and symmetric structure. In early-type bars, the separation of the azimuthal angles of the peaks in the azimuthal profiles in the bar region,

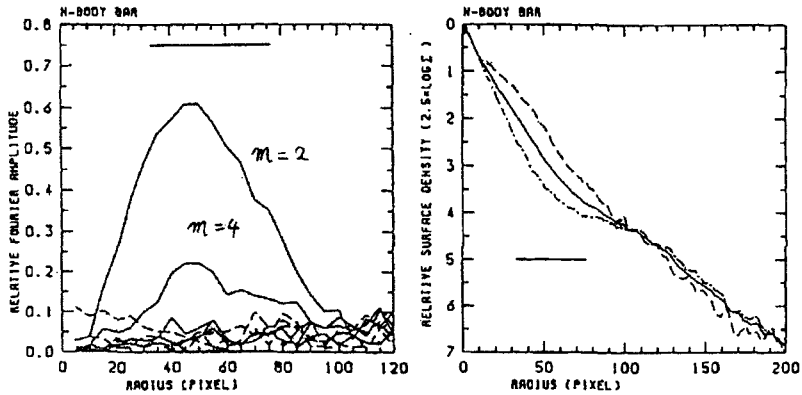


Figure 5. Radial relative Fourier amplitude distribution (left panel) and radial surface density distribution (right panel) of our N-body bar without a bulge component. A horizontal line in each figure represents a bar region. Explanation of the lines is the same as that in Figures 2 and 3.

i.e., straightness of the bar, is almost 180 degree; the deviation from the straight line is about 1 to 2 degrees, which corresponds to 1 to 2 arcseconds and to 1 to 2 pixels of digitizing. So the ridges of the bars are found to show no deviation from a straight line larger than the present detection limit of ± 2 degrees. Bars are very symmetric with respect to the bar major axis; the systematic differences in the luminosity distributions between the leading and trailing sides of the bars are less than 5 to 10% in early-type barred galaxies.

5. Comparison with N-body bars

I would like to compare the observational properties with those of N-body simulations of disks. The model we compare is the same as that in Noguchi (1987) but with a massless perturber. A disk, which is surrounded by a spherical halo of the same mass as the disk, consists of 20,000 particles with an initial surface density of an exponential form and a Q value of 1.

We examine the azimuthal profiles and radial profiles for the N-body bar in quasi-steady state. The relative Fourier amplitudes of the azimuthal profiles is shown in Figure 5. In the bar region, the amplitude of the $m=2$ component is the most dominant component and the second most is the $m=4$ component. However, contributions from higher components are negligible. This property is very similar to the situation for late-type barred galaxies and is quite different from that of early-type barred galaxies.

The radial profiles of the N-body bar are also shown in Figure 5. As can be seen from this figure, the gradient of surface density along the bar major axis is steeper than that in the outer disk region and there is no clear luminosity jump at the bar end. These features are again quite different from those in early-type barred galaxies and are very similar to those of late-type barred galaxies. The

results do not depend on the model of the disk so much if the model does not include a bulge.

However, if the model includes a massive bulge component, the situation changes very much. Combes & Elmegreen (1993) simulated disks with and without a massive bulge component. The resulting radial surface density profiles along the bar major axis and bar minor axis in a less-massive bulge model (their Figure 9) are similar to those in our model and to the observed profiles in late-type barred galaxies. In the model with a massive bulge component, the gradient of the surface density in the bar region is flat as compared with that in the outer disk and some luminosity cut off is seen at the bar end (their Figure 9), though it is not so sharp as the observed one. These features are similar to those in early-type barred galaxies. Thus the properties of a bar presumably depend on the bulge-to-disk mass ratio for a given ratio of bulge-to-disk scale length.

References

- Ann, H. B. 1986, JKAS, 19, 69
Athanasoula, E. & Martinet, L. 1980, A&A, 87, L10
Athanasoula, E., Morin, S., Wozniak, H., Puy, D., Pierce, M. J., Lombard, J., & Bosma, A. 1990, MNRAS, 245, 130
Baumgart, C. W. & Peterson, C. J. 1986, PASP, 98, 56
Benedict, G. F. 1976, AJ, 81, 799
Blackman, C. P. 1983, MNRAS, 202, 379
Buta, R. 1986, ApJS, 61, 631
Buta, R. 1987, ApJS, 64, 383
Combes, F. & Elmegreen, B. G. 1993, A&A, 271, 391
Crane, P. 1975, ApJ, 197, 317
Duval, M. F. & Athanasoula, E. 1983, A&A, 121, 297
Duval, M. F. & Monnet, G. 1985, A&AS, 61, 141
Elmegreen, B. G. & Elmegreen, D. M. 1985, ApJ, 288, 438
Kodaira, K., Watanabe, M., & Okamura, S. 1986, ApJS, 62, 703
Martin, P. 1995, AJ, 109, 2428
Noguchi, M. 1987, MNRAS, 228, 635
Odewahn, S. C. 1991, AJ, 101, 829
Ohta, K., Hamabe, M., & Wakamatsu, K. 1990, ApJ, 357, 71
Okamura, S. 1978, PASJ, 30, 91
Okamura, S. & Takase, B. 1976, Ap&SS, 41, 275
Pence, W. D. & de Vaucouleurs, G. 1985, ApJ, 298, 560
Wozniak, H. & Pierce, M. 1991, A&AS, 88, 325